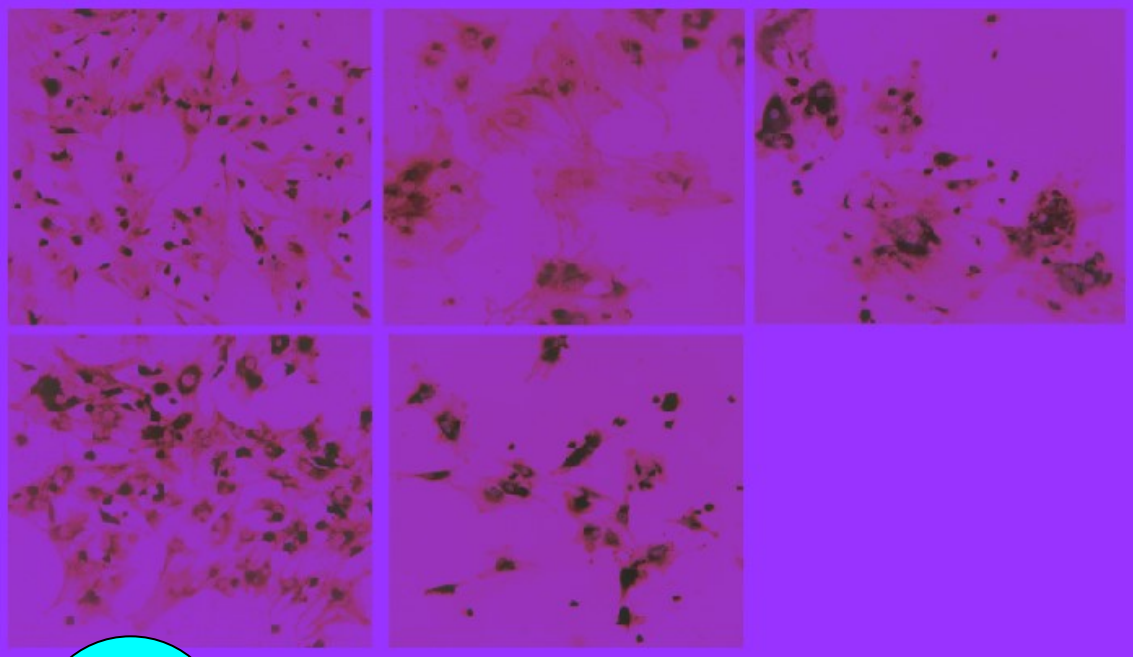

BJP

Bangladesh Journal of Pharmacology

Research Article

# CYT387 restores Th17/Treg cell balance and inhibits mature osteoclast cell formation by regulating SOX-5 signaling in rheumatoid arthritis

A Journal of the Bangladesh Pharmacological Society (BDPS)
Journal homepage: www.bdpsjournal.org; www.banglajol.info
Abstracted/indexed in Academic Search Complete, Agroforestry Abstracts, Asia Journals Online, Bangladesh Journals Online, Biological Abstracts, BIOSIS Previews, CAB Abstracts, Current Abstracts, Directory of Open Access Journals, EMBASE/Excerpta Medica, Global Health, Google Scholar, HINARI (WHO), International Pharmaceutical Abstracts, Open J-gate, Science Citation Index Expanded, SCOPUS and Social Sciences Citation Index
**Bangladesh J Pharmacol 2023; 18: 138-151**
**ISSN**: 1991-0088

# CYT387 restores Th17/Treg cell balance and inhibits mature osteoclast cell formation by regulating SOX-5 signaling in rheumatoid arthritis

**Susmita Srivastava and Mahaboobkhan Rasool**

*Immunopathology Lab, School of Biosciences and Technology, Vellore Institute of Technology, Vellore 632 014, Tamil Nadu, India.*

## Article Info

Received: 21 September 2023
Accepted: 1 October 2023
Available Online: 17 December 2023
DOI: 10.3329/bjp.v18i4.68901

Cite this article:
Srivastava S, Rasool M. CYT387 restores Th17/Treg cell balance and inhibits mature osteoclast cell formation by regulating SOX-5 signaling in rheumatoid arthritis. Bangladesh J Pharmacol. 2023; 18: 138-51.

## Abstract

The present study was conducted to investigate the therapeutic efficacy of CYT387 in rheumatoid arthritis pathogenesis concerning T helper 17 cell/ regulatory T cell (Th17/Treg) imbalance and osteoclastogenesis. In this study, CYT 387 inhibited the proliferation of Th17 cells and collectively relocated FoxP3 + Treg cell differentiation *in vitro*. CYT387 mitigated the secretion of pathogenic IL-17 via reduced ROR-γt expression and restored the elevated expression of IL-10 by increasing FOXP3 activity. Alternatively, CYT387 abrogated RANKL expression and significantly increased osteoprotegerin levels by reducing SOX-5 activity. Furthermore, in a co-culture system of IL-6 and sIL-6R stimulated adjuvant-induced arthritic fibroblast-like synoviocytes and monocytes/macrophages collected from rat bone marrow, CYT387 reduced osteoclast formation and bone resorptive activity. In conclusion, CYT387 modulated IL-6/sIL-6R dependent JAK1/STAT3 activation and signaling mechanisms in CD4+T cells under Th17 differentiation conditions and osteoclast cells via dampened activation of SOX-5.

## Introduction

Rheumatoid arthritis is a musculoskeletal autoimmune disorder that is well-interplayed and methodically managed by a network of innate and adaptive immune cells centered at the synovial joint (McInnes et al., 2016; Kondo et al., 2021). These cellular components infiltrate the synovium and communicate further, resulting in increased production of cytokines that favor inflammation and pannus development, causing irreversible joint deformity. Among these, extensive studies have elucidated the delirious involvement of T cells as crucial cellular components in perpetuating the pathophysiology of rheumatoid arthritis (Toh and Miossec, 2007).

Convincing reports have established the detrimental role of interleukin-6 (IL-6), an indispensable cytokine in the lineage commitment of inflammatory T helper 17 (Th17) cells from CD4+ T cells (Van Hamburg and Tas 2018). In the presence of a descent-specific transcriptional factor, retinoic-acid-related orphan nuclear receptor (RORγT), this pathogenic variant of T cells perpetuates the disease via the profound release of inflammation-mediating interleukin-17 (IL-17) cytokines (Kotake et al., 2017). In line with IL-6, interleukin-23 (IL-23) interacts with interleukin-23R (IL-23R) and maintains clonal expansion of the cell. This clonal propagation later promotes the release of various inflammatory mediators involved in bone and cartilage destruction (Kim et al., 2013). However, this increased percentage of Th17 cells is compensated for by decreased regulatory T cell (Treg) differentiation (Noack and Miossec, 2014). Elevated IL-6 levels in the rheumatoid synovium distort the Th17/Treg balance and consequently inhibit the activation of forkhead box P3

(FOXP3), causing a scarcity of autoimmunity resisting regulatory T cells via abated IL-10 expression (Jiang et al., 2021). A dysregulated Th17/Treg cell balance appears crucial in demonstrating a constellation of rheumatoid arthritis symptoms (Kimura and Kishimoto, 2010; Bin Dhuban et al., 2019). As a result, Th17/Treg cell imbalance serves as a prime hotspot for validating crucial targets in rheumatoid arthritis.

In addition to the disproportionate stability of Th17 and Treg cells, IL-6-driven bone resorption activity and osteoclastogenesis via up-regulation of receptor activator of nuclear factor κB ligand (RANKL) and shrunken osteoprotegerin levels are also one of the indicated features of rheumatoid arthritis (Wu et al., 2017). RANKL, an evaluative marker of bone damage released from fibroblast-like synoviocyte (FLS) cells, interacts with the receptor RANK exhibited on the precursor osteoclast cells. This interaction enhances the formation of tartrate-resistant acid phosphatase (TRAP+) osteoclast cells, which enhance bone resorption activity in rheumatoid joints (Hashizume et al., 2008).

Intriguingly, under inflammatory conditions, IL-6 initiates trans-signaling with its soluble receptor (sIL-6R) and significantly increases Th17 cell differentiation. Moreover, cells such as FLS also mediate pro-inflammatory activities in the rheumatoid arthritis synovium via IL-6 trans-signaling. Later, this IL-6/sIL-6R complex aberrantly activates the JAK/STAT path-way and finally constrains immune responses (Jones et al., 2010). However, the increased functionality of T cells is also attributed to IL-6-mediated unrestrained activation of the JAK/STAT-3 signaling cassette. Fur-ther scientific studies have confirmed STAT-3 modulated genetic changes in CD4+T cells, which causes differentiation into the pathogenic phenotype, Th17 (Yang et al., 2007). Studies have also demonstrated the formation of a high number of Th17 cells via JAK-1 activation upon downregulation of suppressor of cytokine signaling (SOCS)-3. SOCS-3, a negative feed-back inhibitor of the JAK/STAT pathway, regulates signaling magnitude (Chen et al., 2015). Nevertheless, the exact mechanism of activation of the downstream targets of IL-6/sIL-6R/JAK-1/STAT-3 responsible for Th17-derived pathogenicity and osteoclastogenesis has not been clearly defined. c-Maf and SOX-5 were up-regulated in the IL-6 microenvironment. Subsequently, this complex induces RORγT expression and plays a significant role in Th17 differentiation, thus contributing to diverse pathologies in rheumatoid arthritis (Tanaka et al., 2014). Consequently, scientific data reveals that SOX-5 in an IL-6/sIL-6R environment shows a stronger affinity for the RANKL promoter (Feng et al., 2016). Collectively, these data revived the interest in studying IL-6 trans-signaling and SOX-5 mediated abnormalities within the rheumatoid arthritis microenvironment. Moreover, establishing the molecular mechanism linking SOX-5 with Th17 cell differentiation and osteoclast formation in an IL-6/sIL-6R-dependent manner might help decode a novel therapeutic strategy to cure rheumatoid arthritis.

Currently, agents in the armamentarium are small molecular inhibitors that target the JAK/STAT signaling axis and have greatly expanded the spectrum of treatment strategies. Among them, a Janus kinase small molecule inhibitor, momelotinib (CYT387), has been shown to compete with JAK-1/JAK-2 for ATP binding, resulting in JAK1/2 inactivation (Tefferi et al., 2018). CYT387 has also been extensively studied for its anti-cancer properties. Consistent with this, CYT387 also halted the ACVR1-hepcidin axis, which mitigated hepcidin and iron levels, causing a significant improvement in rheumatoid arthritis-linked anemia in an arthritic rat model (Tymoszuk et al., 2020). Importantly, in murine models of myeloproliferative neoplasms, CYT387 abrogates the secretion of inflammatory cytokines (Gupta et al., 2017; Verstovsek et al., 2021). In connection with these findings, the previous report from our lab substantiated the anti-arthritic capacity of CYT387 in an adjuvant-induced arthritic rat model of rheumatoid arthritis (Srivastava et al., 2021). Presumably, no mechanistic validation exists for CYT387 anti-inflammatory and anti-arthritic efficacy in modulating IL-6/sIL-6R, an arbitrated pathological function of IL-17-secreting Th17 cells. Moreover, CYT387 efficiency of RANKL-mediated osteoclastogenesis remains unexplored. Therefore, the current study aimed to elucidate the therapeutic capability of CYT387 in restoring the Th17/Treg balance, as well as an anti-bone resorptive agent, to further explore the rudimentary mechanism of action of CYT387 in rheumatoid arthritis.

## Materials and Methods

### *Reagents*

MedChem Express (USA) provided CYT387 (momelotinib) and S3I-201, a STAT-3 inhibitor. Interleukin- 6 (IL -6) was purchased from Immunotools, and its soluble IL -6 receptor (sIL-6R) was obtained from Peprotech. Fetal bovine serum (FBS), antibiotic solution, collagenase of type II, and Dulbecco's modified Eagle's medium (DMEM) were provided by Sigma-Aldrich, USA. Primary antibodies against JAK-1, STAT-3, p-JAK-1, p-STAT-3, IL-23R, c-Maf, SOCS-3, SOX-5, RANKL, IL-17, and β-actin, and anti-rabbit secondary antibody conjugated with HRP were acquired from ABclonal (USA). RORγT and FOXP3 were obtained from BioLegend. Santacruz Biotechnology provided the anti-IL-10 and anti-osteoprotegerin primary antibodies.

### *Animal model*

Wistar albino rats (n = 6) of either sex were used in this experiment. The animals were provided by the in-house animal facility at the Vellore Institute of Technology,

India. The animals were 8-10 weeks weighing around (150-180 g). To minimize stress-related behavior, animals were housed in a compatible pair. These experimental animals were primarily housed in cages with smooth surfaces and minimal angles and edges to avoid accumulating dirt and debris and facilitate sanitation. The animals were kept under a cycle of 12 hours of light and dark at controlled temperatures ranging between 22 and 24°C in a clean environment. Before the experiment, the animals were given the recommended rodent food along with water.

After acclimatization, arthritis was induced using complete Freund's adjuvant (Sigma-Aldrich, USA) in experimental animals. Complete Freund's adjuvant was suspended at a concentration of 10 mg/mL in sterile paraffin oil and intradermally injected into the right footpad of experimental rats. Body weight and paw thickness were assessed periodically to determine disease severity.

***Isolation of CD4+T cells***

On the 21st day after induction, the animals were sacrificed via cervical dislocation. CD4+ T cells were isolated from the spleen and lymph nodes of adjuvant-induced arthritic rats using the EasySep™ kit, according to the manufacturer's protocol (STEMCELL Technologies, Canada). The cells were later stimulated with anti-CD3 (0.5 µg/mL) and anti-CD28 (1 µg/mL) (BD Biosciences, USA). Roswell Park Memorial Institute 1640 medium (Sigma-Aldrich, USA) was used to culture the cells for future analysis. Brefeldin A (10 µg/mL) (BioLegend, USA) treatment for 4 hours was used to inhibit the secretion of cytokines. For differentiation of Th17 cells, splenocytes were stimulated with TGF-β (2 ng/mL) and IL-6 or IL-6/sIL-6R (20 ng/mL) microenvironment followed by IL-23 (6 ng/mL) stimulation.

***Purity analysis of CD4+ T cells***

Isolated T cells from the spleen and lymph nodes of arthritis-induced rats were assessed for purity by staining for specific CD4 cell surface markers. The isolated T cells were trypsinized and washed with freezing flow cytometry staining buffer (FACS buffer) (1% BSA in PBS). Further, the cells were incubated in the dark for 30 min at 4°C with FITC conjugated CD4+ antibody (BioLegend, USA). Stained cells were analyzed using a CytoFLEX Flow Cytometer (Beckman Coulter, USA).

***MTT Assay***

Isolated adjuvant-induced arthritic (AA) CD4+T cells seeded in 96 well plates were treated with CYT387 at dosages ranging between 0.1 -2 µM. Dimethyl sulfoxide at a 100% concentration was used as a positive control. Following incubation for 24 hours, 3-(4,5-dimethylthiazolyl)-2,5-diphenyltetrazolium bromide (MTT) (Sigma) (20 µL/well) stock reagent (5 mg/mL dissolved in PBS) was added and incubated for 4 hours. After incubation, formazan crystals were solubilized by adding 100 µL dimethyl sulfoxide. The absorbance was read at 570 nm. The live cells treated with CYT387 at different concentrations are shown as percentages compared to 100% of the control value.

***Primary culture of isolated fibroblast-like synoviocytes (FLS) cells***

FLS cells were isolated from normal and adjuvant-induced arthritic (AA) rats after inducing 0.1 mL of complete Freund's adjuvant. Until the 20th day, the severity of the disease was recorded systematically. On day 21, after examination, the knee joints were excised from the experimental rats and dissected to obtain synovial tissues in a clean environment. After dissection, a single-cell suspension was obtained by enzymetic digestion with 0.4% type II collagenase in DMEM supplemented with 5% FBS at 37°C for 4 hours. After incubation, the cell suspension was centrifuged and the pellet was resuspended in DMEM supplemented with 10% FBS, 100 units/mL penicillin and 100 µg/mL streptomycin. Subsequently, the cells were incubated in a T25 culture flask in a humidified $CO_2$ incubator at 37°C. The following day, the floating cells were removed, and the adherent cells were given prior conditions, as stated. FLS cells between passage numbers 5 and 9 were used for further experimentation.

***Purity analysis of AA-FLS cells***

FLS cells isolated from experimental arthritis rats were screened for purity by evaluating the expression of the surface marker CD90.2. At the fourth passage, the isolated AA-FLS cells were trypsinized and washed with freezing FACS buffer (1% BSA in PBS). Following washing, the cells were kept in the dark for 30 min at 4°C with FITC-conjugated CD 90.2 monoclonal antibody obtained from Biolegend (USA). Finally, the stained cells were analyzed for CD90.2.

***In vitro cell culture treatment***

CD4+T cells collected from the spleen and lymph nodes of arthritis-induced rats were stimulated with Th17-polarizing conditions of IL-6 or IL-6/ sIL-6R, TGF-β, IL-23 for 72 hours. After 72 hours incubation, the cells were treated with different doses (0.25 and 0.75 µM) of CYT387 or left untreated for the next 24 hours. Unless otherwise mentioned, S3I-201 (50 µM), a STAT3 inhibitor, was added to cells before IL-6/ sIL-6R stimulation. To study osteoclastogenesis, AA-FLS were stimulated with or without IL-6/sIL-6R (100 ng/mL) for 24 hours. After stimulation, cells were treated with CYT387 (0.25 and 0.75 µM) or left untreated for another 24 hours. S3I-201 (50 µM), a STAT3 inhibitor, was added to the cells 24 hours prior to IL-6/sIL-6R stimulation. Similarly, treated AA-FLS cells were co-cultured with bone marrow-derived macrophages for TRAP and pit assays.

***Western blot analysis***

After treatment, the cells were harvested and lysed using cold radioimmunoprecipitation assay buffer with a protease inhibitor cocktail (Sigma, USA). The Bradford kit (Bio-Rad, USA) was used to estimate total protein levels. The lysate (30 µg per lane) was then electrotransferred onto polyvinylidene difluoride membranes (Amersham Pharmacia Biotech, Sweden) using a transblot turbo, a semi-dry transfer unit (Bio-Rad, USA) within 20 min of being subjected to sodium dodecyl sulfate-polyacrylamide gel electrophoresis. The transfer of protein lysate was confirmed by incubating the polyvinylidene difluoride membrane with Ponceau staining for 5 min. Following transfer confirmation via staining, the membranes were kept overnight in a blocking buffer (5% BSA prepared in tris-buffered saline tween-20 (TBST) at 4°C. Subsequently, the membranes were incubated with targeted primary antibodies overnight at 4°C and then incubated for 2 hours at room temperature with HRP-conjugated secondary antibody (1:10,000 dilution). Specific primary antibodies to total JAK-1, total STAT-3, phosphorylated JAK-1, phosphorylated STAT-3, c-Maf, IL-23R, SOX-5, SOCS-3, IL-17, IL-10, RORγT, FOXP3, RANKL, osteoprotegerin, and β-actin were used. After incubation using the improved chemiluminescence solution from Millipore (USA), the membranes were developed and photographed using a gel documentation system (Bio-Rad, USA). The expression of all proteins was normalized to their respective totals, β-actin, and quantified using Image J software [version 1.48 (Wayne Rasband, USA)].

### *Real-time polymerase chain reaction (qRT-PCR) analysis*

TRIzol reagent (Sigma-Aldrich) was used to extract the entire RNA according to the manufacturer's protocol. cDNA was synthesized using a reverse transcription 326 cDNA kit (Applied Biosystems, USA). Subsequently, cDNA was analyzed using an EvaGreen Supermix PCR kit (Bio-Rad, USA). The NCBI primer BLAST tool was used to design the primers. Sigma Aldrich, USA provided the designed primers. The cycling conditions required for qRT-PCR analysis were as follows: 95°C for 15 min, followed by 94°C for 15 sec, then 40 cycles of 60°C for 30 sec, and finally 72°C for 30 sec. The relative expression levels of the specified genes were normalized to GAPDH using the 2-ΔΔCt method.

### *Isolation of bone marrow-derived macrophages*

Bone marrow-derived macrophages with diminutive changes were obtained from Wistar albino rats, as previously mentioned. Briefly, the long femur bones were excised and the entire bone marrow was drained using a 25-G needle onto a sterile petri plate containing 5 mL of DMEM. Red blood lysis buffer for 30 sec at 37° C to remove red blood cells, followed by centrifugation. The collected cells were suspended in DMEM supplemented with 10% FBS, 25 ng/mL macrophage colony-stimulating factor along 2 mM L-glutamine, 100 U/mL penicillin, and 100 µg/mL streptomycin for three days.

### *Staining for TRAP+ osteoclast cells*

For osteoclast differentiation, AA-FLS cells, post-treated with/without CYT387 (0.25 and 0.75 µM) and pre-treated with S3I-201 (50 µM), respectively, for 24 hours after stimulation or with/without IL-6/sIL-6R (100 ng/mL) for 24 hours co-cultured for 7 days with rat bone marrow-derived macrophages in quantity tissue cultures plates. After 7 days of incubation, TRAP+ osteoclast cells were observed using an acid phosphatase leukocyte kit (Sigma-Aldrich), according to the manufacturer's instructions. TRAP+ multinucleated cells with more than three nuclei were taken as mature osteoclasts and quantified at 40x magnification using an inverted microscope (Olympus America, USA). Three random areas in each group were visualized at 10x magnification for TRAP+ osteoclast cells to represent graphically.

### *Pit formation assay*

AA-FLS cells, post-treated with/without CYT387 (0.25 and 0.75µM) and pre-treated with S3I-201 (50 µM), respectively, for 24 hours after stimulation with/without IL-6/sIL-6R (100 ng/mL) for 24 hours were cocultured with rat bone marrow-derived macrophages in corning osteo-assay surface 24-well plate. The plate provides a smooth mineralized surface that mimics the bone material. After 7 days of co-culture, the cells were exhausted by incubating with 100 µL of 5% sodium hypochlorite for 5 min and kept at room temperature. The plates were then washed twice with PBS and dried for 5 hours. An inverted microscope (Olympus, USA) at 40x magnification was used to capture the resorption pits formed by functionally mature osteoclasts. The number of resorption pits in three different areas was counted and averaged.

### *Statistical analysis*

Data from three independent experiments are presented as mean ± standard error of the mean (SEM). For significant statistical differences between different experimental groups, one-way analysis of variance (ANOVA) was performed, followed by Bonferroni multiple comparison post-test. Statistical analysis was performed using SPSS software (version 15.0; IBM SPSS Statistics, USA) to check for statistical analysis where a p-value ≤0.05 was taken as statistically significant.

## Results

### *CYT387 on arthritic CD4+T cell viability*

CD 4 + T cells were isolated from the spleen and lymph nodes of arthritis-induced rats using the EasySep™ rat CD4+T cell isolation kit (STEMCELL Technologies, Canada) as per the manufacturer's procedure. Following isolation, the cells were analyzed using flow cytometry to determine the purity of the CD4 markers and

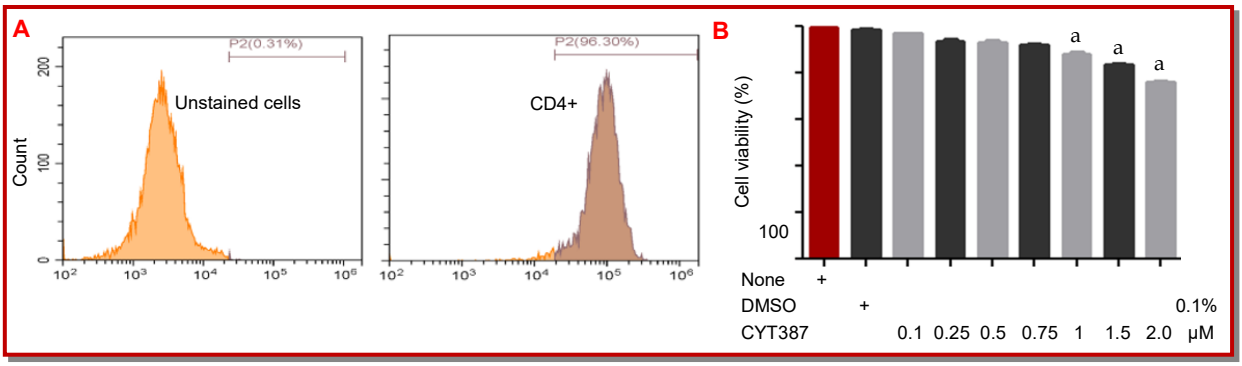


Figure 1: Effect of CYT387 treatment on CD4+ T-cell viability. CD4+ T cells were analyzed using flow cytometry to determine the purity of the CD4 markers (A). The viability of arthritic CD4+ T cells following treatment with the indicated concentrations of CYT387 for 24 hours was estimated using MTT assay (B). All error bars represent the mean ± SEM (n=3). [a]p<0.001 compared to control

the results demonstrated ≥95% stained positive for the CD4+T cell population (Figure 1A). The MTT assay determined the cytotoxicity of CYT387 on adjuvant-induced arthritic (AA) CD4+T cell viability after treatment for 24 hours. CYT387 concentration between 0.1 to 0.75 μM did not critically influence the viability of arthritic CD4+T cells. However, treatment with a higher level of CYT387 ≥0.75 μM markedly reduced the viability of arthritic CD4 + T cells ($p<0.001$) (Figure 1B). Therefore, for further experiments, CYT387 concentrations of 0.25 and 0.75 μM were selected.

### *Effect of CYT387 on Th17/Treg cell-related cytokines*

To determine the inhibitory mechanism of CYT387 at the *in vitro* level on Th17 differentiation, isolated arthritis CD4+ T cells from the spleen and lymph nodes were grown in a Th17- differentiation environment of IL-6 or (IL-6/sIL-6R), TGFβ, IL-23 for 72 hours and later treated for 24 hours in the presence and absence of CYT387. sIL-6R stimulation along with Th17 skewing conditions in CD4+ T cells increased the levels of IL-17 and reduced the levels of IL-10 compared with cells under Th17 skewing conditions of IL-6, TGFβ, and IL-23 only. However, CYT387 at a higher concentration (0.75 μM) notably modulated the expression of Th17/Treg cell-related cytokines at both the mRNA and protein levels. To confirm differentiation, IL-17 mRNA showed reduced expression, whereas IL-10 mRNA levels were increased under the given conditions (Figure 2A). Likewise, the protein level of IL-17 demons-trated a similar decrease with elevated IL-10 protein levels (Figure 2B). Similarly, S3I-201 (STAT-3) inhibitor treatment demonstrated results similar to those observed for CYT387 at 0.75 μM dosage.

### *Effect of CYT387 on Th17/T reg cell differentiation*

A skewed Th17/Treg cell balance has been implicated in disease progression and maintenance of inflammation. RORγT, a master transcription factor, is over-expressed under Th17 differentiation conditions (Kimura and Kishimoto, 2010). As shown in Figure 3, sIL-6R stimulation along with Th17 skewing conditions in CD4+ T cells from experimental arthritis rats increased the activation of RORγT when compared with cells stimulated with Th17 skewing conditions of IL-6, TGFβ, and IL-23 only. Interestingly, CYT387 treat-ment at 0.75 μM dosage exhibited the maximum inhibitory capacity on RORγT activation downstream of IL-6 trans-signaling and further promoted the differentiation of FOXP3 Treg cells. To confirm the differentiation of Treg cells, the mRNA (Figure 3A) and protein (Figure 3B) levels of FOXP3 were estimated. In sIL-6R stimulated group with Th17 differentiation, there was a decline in FOXP3 levels when compared to the cells stimulated with Th17 skewing conditions of IL-6, TGFβ, IL-23 only and CYT387 treated groups. CYT387 at a higher dose (0.75 μM upregulated FOXP3 mRNA and protein expression inside the cell. Correspondingly, S3I-201 (STAT-3 inhibitor) reduced RORγT and elevated FOXP3 mRNA and protein expression like CYT 387 at 0.75 μM concentration.

### *CYT387 inhibits IL-6/sIL-6R mediated IL-23R expression*

The expression of Th17-related molecule, IL-23R in response to sIL-6R and Th17 polarizing conditions was analyzed. However, to determine whether CYT387 can enervate the IL-6/sIL-6R regulated level of IL-23R, isolated CD4+ T cells from experimental arthritis rats were stimulated with sIL-6R along with Th17 inclining conditions and subsequently dosed with varying concentrations of CYT387. As shown in Figure 4, sIL-6R stimulation of T cells under Th17 differentiation conditions increased the expression of IL-23R when compared with the traditional Th17 polarizing conditions of IL-6, TGFβ, and IL-23 only. Principally, a higher dose of CYT387 (0.75 μM) declined IL-23R protein expression as evidenced by western blot analysis. Simultaneously, the STAT-3 inhibitor showed similar results as CYT387 at 0.75 μM concentration.

### *Role of CYT387 in IL-6/sIL-6R modified JAK-1/ STAT-3 activation in arthritic CD4+T cells*

To understand the elementary mechanism at the

molecular level through which CYT387 attenuates CD4+ T cell differentiation to Th17, IL-6/sIL-6R was used to regulate the JAK-1/STAT-3 signaling pathway. As shown in Figure 4, sIL-6R stimulation of isolated CD4+T cells from arthritis-induced rats under Th17 differentiation conditions increased the phosphorylation of activated JAK-1 compared with cells under traditional Th17 polarizing conditions of IL-6, TGFβ, and IL-23 only. Interestingly, treatment with CYT387 (0.75 µM) abrogated JAK-1 phosphorylation, as shown by immunoblotting. Moreover, CYT387 treatment heightened the levels of SOCS-3. This later inhibited STAT-3 activation. Next, the expression of total and phosphorylated STAT-3 was evaluated. As calculated, the magnitude of phosphorylated STAT-3 was incremented in sIL-6R stimulated CD4+ T cells cultured under Th17 differentiating conditions compared with cells under Th17 differentiation conditions of IL-6, TGFβ, and IL-23 only. Remarkably, post-treatment with CYT387 reduced STAT-3 phosphorylation and its subsequent expression. Similarly, treatment with S3I-201 abrogated the activation of STAT-3.

### *CYT387 modulates Th17/Treg cell balance via c-Maf - SOX-5 activation in arthritic CD4+ T cells*

SOX-5 and c-Maf play critical roles in the differentiation of the Th17 subset, and subsequently act as critical downstream effector molecules of the JAK-1/STAT3

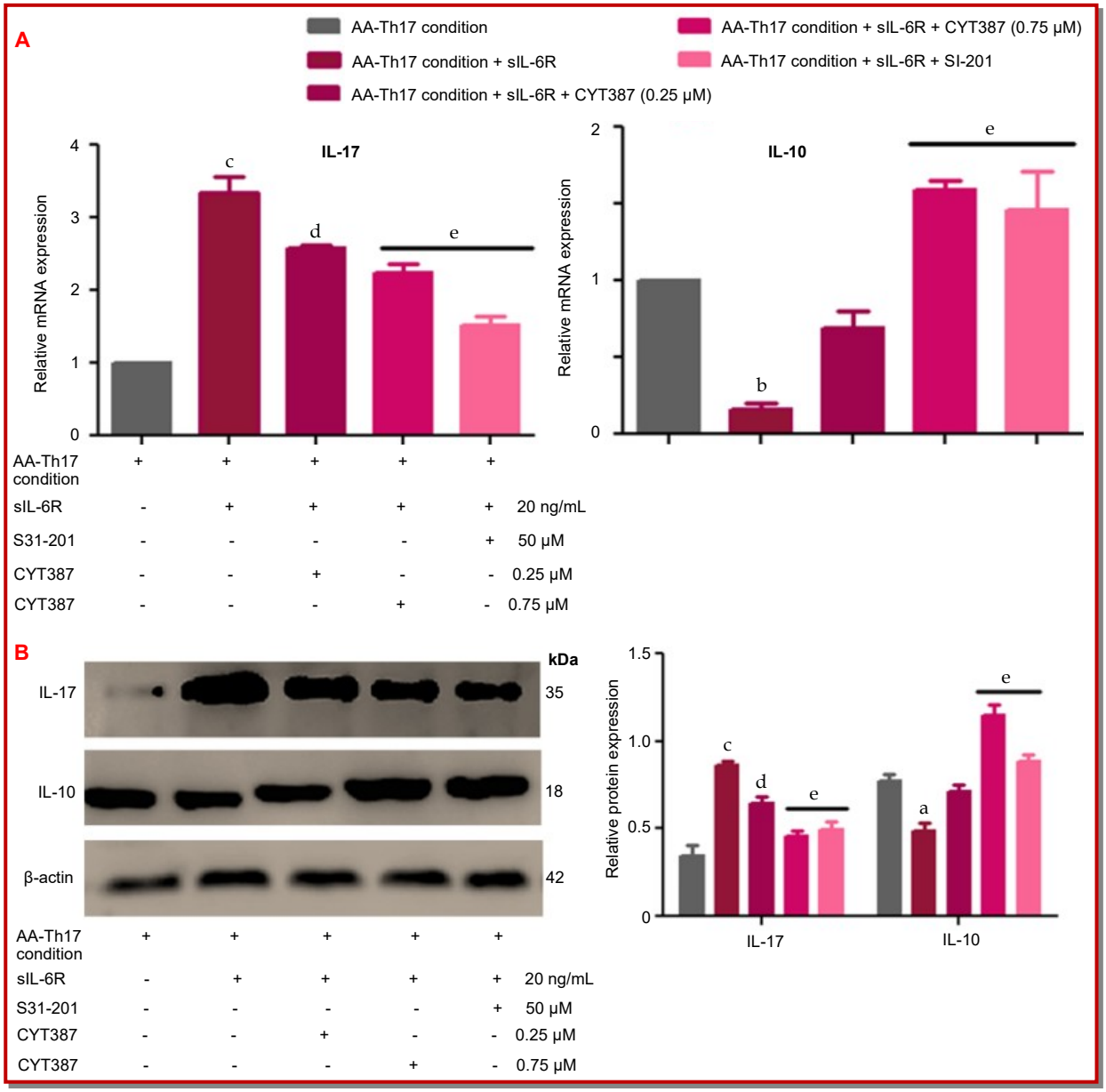


Figure 2: Effect of CYT387 on Th17/Treg cell related cytokines. The mRNA expression of IL-17and IL-10 were analyzed using quantitative real-time PCR (A). Western blot analysis was performed to detect IL-17 and IL-10 protein expression (B). All error bars represent the mean ± SEM (n=3). [a]p<0.05; [b]p<0.01; [c]p<0.001, compared to arthritis CD4+T cells under Th17 differentiation condition. [d]p<0.05; [e]p<0.001 compared with sIL-6R stimulated arthritis

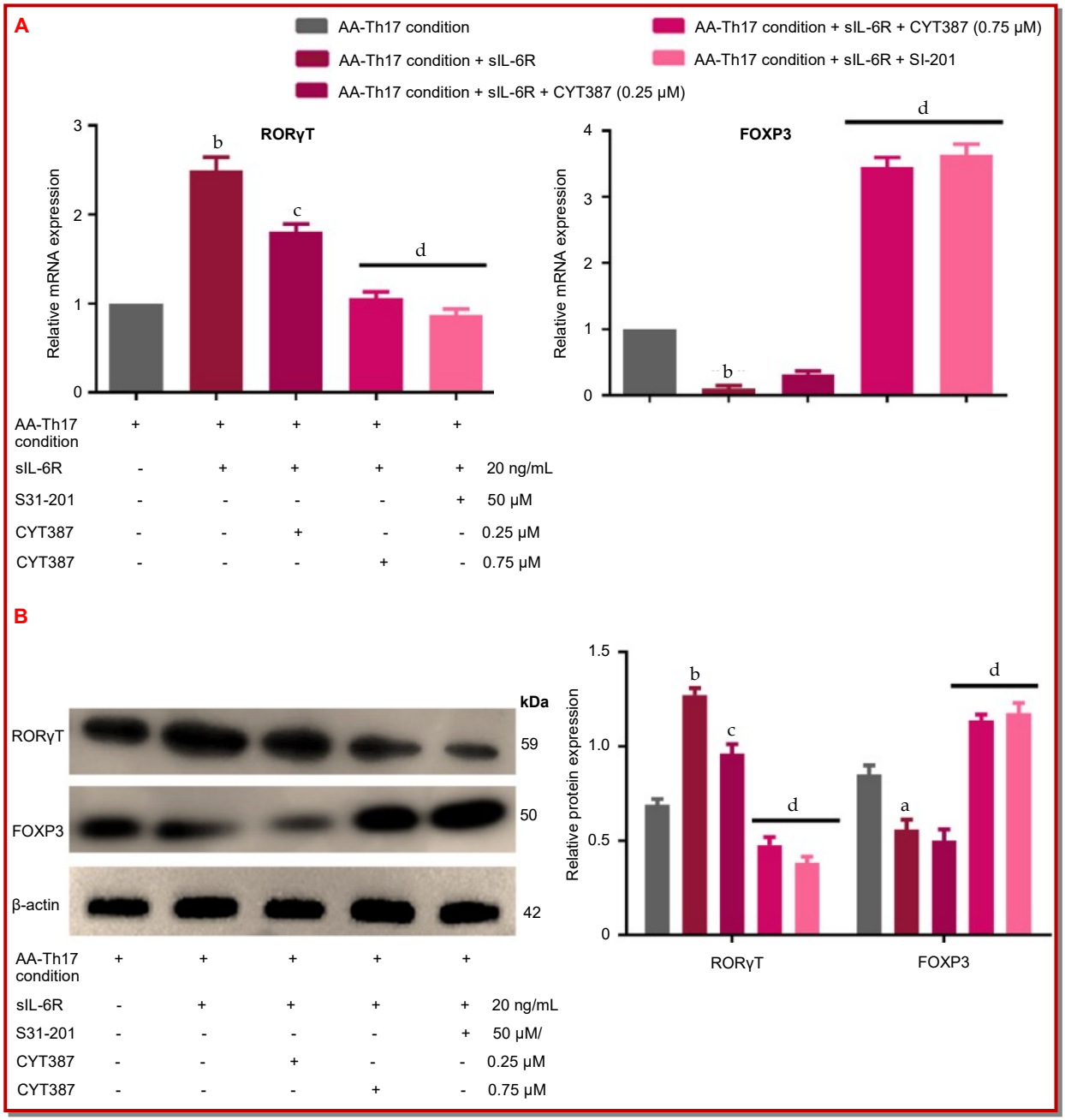


Figure 3: Effect of CYT387 on Th17/Treg cell differentiation. mRNA expression of RORγT and FOXP3 was analyzed using quantitative real-time PCR (A). Western blot analysis was performed to detect protein expression of RORγT and FOXP3 (B). All error bars represent the mean ± SEM (n=3). [a]p<0.05; [b]p<0.001, compared to arthritis CD4+T cells under Th17 differentiation condition. [c]p<0.01; [d]p<0.001 compared with sIL-6R stimulated arthritis CD4+T cells under Th17 differentiation conditions. sIL-6R; soluble Interleukin-6 receptor, CD, cluster of differentiation; Th17, T helper 17; Treg, regulatory T cell; RORγT, RAR-related orphan receptor gamma; FOXP3, Forkhead box P3

pathway in distorting the Th17/Treg imbalance (Tanaka et al., 2014). In the present study, a corresponding increase in the quantity of c-Maf and SOX-5 (Figure 4) proteins was observed in CD4+T cells isolated from arthritis-induced rats stimulated with sIL-6R along with Th17 polarizing conditions when compared to cells stimulated only under Th17 polarizing conditions of IL-6, TGFβ, and IL-23 only. However, CYT387 treatment (0.75 μM) resulted in reduced levels of c-Maf and SOX-5 in T-cells. This was concomitant with the activity of S31-201 (STAT3) inhibitor.

### *CYT387 abates IL-6/sIL-6R modulated osteoclast formation and bone resorption in AA-FLS cells*

RANKL and its receptor RANK transform osteoclast precursors, macrophages, into multinucleated TRAP+

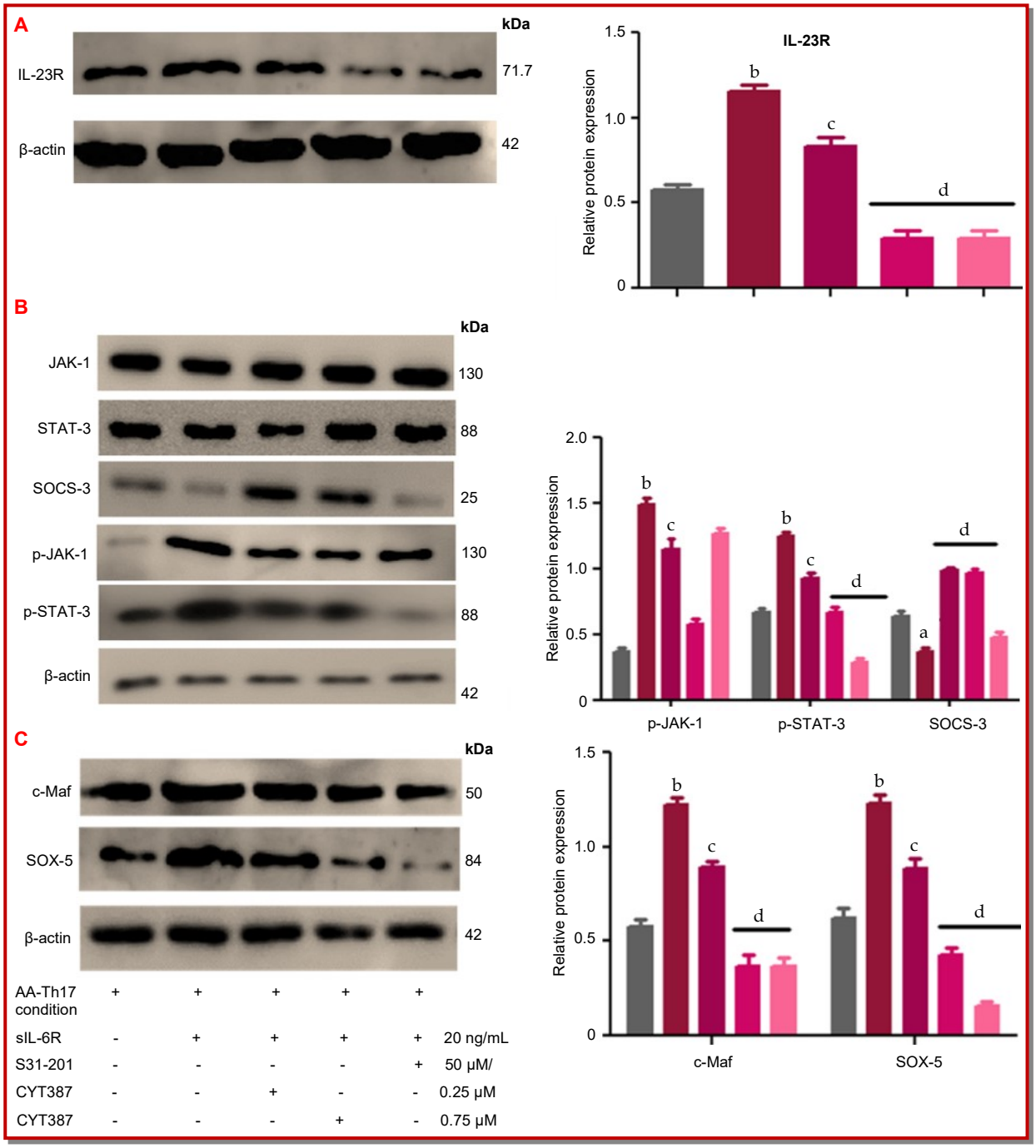


Figure 4: Effect of CYT387 on IL-23R expression (A), JAK-1/STAT-3 signaling cascade (B), and c-Maf-SOX-5 signaling in regulating Th17/Treg cell balance (C) *in vitro*. All error bars represent the mean ± SEM (n=3). [a]p<0.01; [b]p<0.001, compared to arthritis CD4+T cells under Th17 differentiation condition. [c]p<0.01; [d]p<0.001 compared with sIL-6R stimulated arthritis CD4+T cells under Th17 differentiation conditions. sIL-6R; soluble interleukin-6 receptor, CD, cluster of differentiation; Th17, T helper 17; IL-23R; Interleukin 23 Receptor, Treg: regulatory T cell; JAK: Janus activated kinase; STAT: signal transducer and activator of transcription factors; SOCS-3: suppressor of cytokine signaling 3; soluble interleukin-6 receptor, SOX-5; SRY-Box transcription factor 5

osteoclast cells and induce bone erosion in rheumatoid joints. IL-6/sIL-6R demonstrates osteoclastogenic potential by inducing the abundant release of RANKL by FLS cells in patients with rheumatoid arthritis (Hashizume et al., 2008). Accordingly, to explore the effectiveness of CYT387 in inhibiting osteoclast formation upon IL-6 and sIL-6R stimulation, the isolated AA-FLS cells were phenotypically characterized. Upon purity analysis, the specific FLS cell surface marker CD90.2 (Figure 5), co-culturing of cells was initiated. Thereafter,

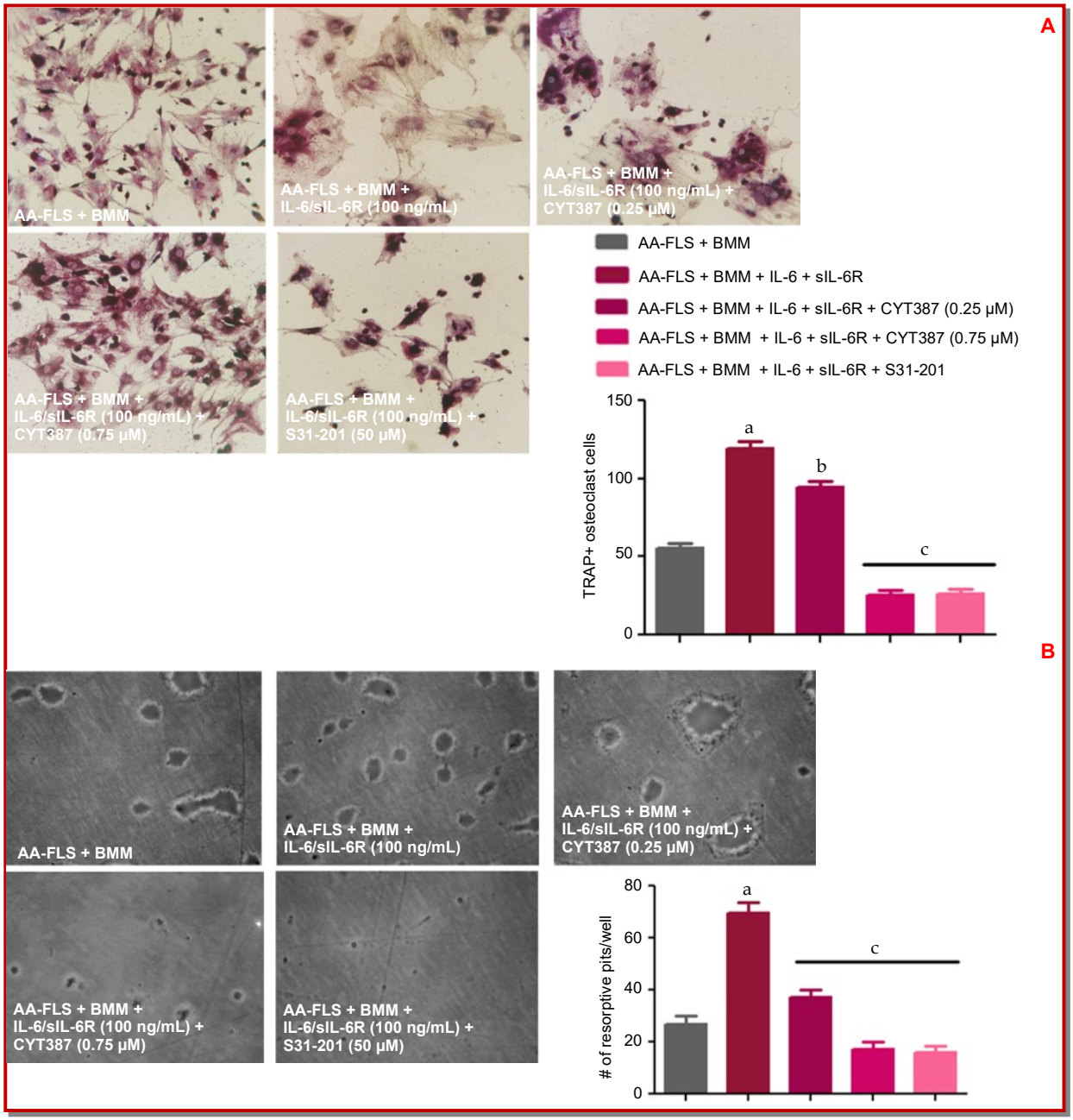


Figure 5: IL-6/sIL-6R modulated osteoclast formation and bone resorption in AA-FLS upon CYT387 treatment. TRAP+ multinucleated cells containing three or more nuclei were marked as osteoclasts and counted using an inverted microscope. Magnification: 40x; Scale Bar: 20 µm (A). Bone resorption pits formed on the osteo assay plates were counted, and images were taken (Magnification: 20x) using an inverted microscope (B). All error bars represent the mean ± SEM (n=3). [a]p<0.001, compared with disease control AA-FLS+ bone marrow-derived macrophages cells. [b]p<0.01; [c]p< 0.001 compared to AA-FLS+ bone marrow-derived macrophages cells stimulated with IL-6/sIL-6R. IL-6; interleukin- 6, sIL-6R; soluble interleukin-6 receptor, AA-FLS, adjuvant-induced arthritis fibroblast-like synoviocytes; TRAP, tartrate-resistant acid phosphatase; BMM: bone marrow-derived macrophages

the osteoclast precursor cells were co-cultured with AA -FLS and AA-FLS stimulated with IL-6/sIL-6R, IL-6, and sIL-6R induced AA-FLS post-treatment with CYT387 and IL-6 along with sIL-6R stimulated AA-FLS where STAT-3 function was halted by the STAT-3 inhibitor, S3I-201.

After a week of co-culture, an increased number of TRAP+ polynuclear osteoclasts cells was determined by TRAP staining assay in AA-FLS cells activated with IL-6/sIL-6R. Treatment with CYT387 (0.75 µM) mitigated IL-6 and sIL-6R-mediated osteoclastogenesis, as evidenced by the decreased number of TRAP+ osteoclasts. In

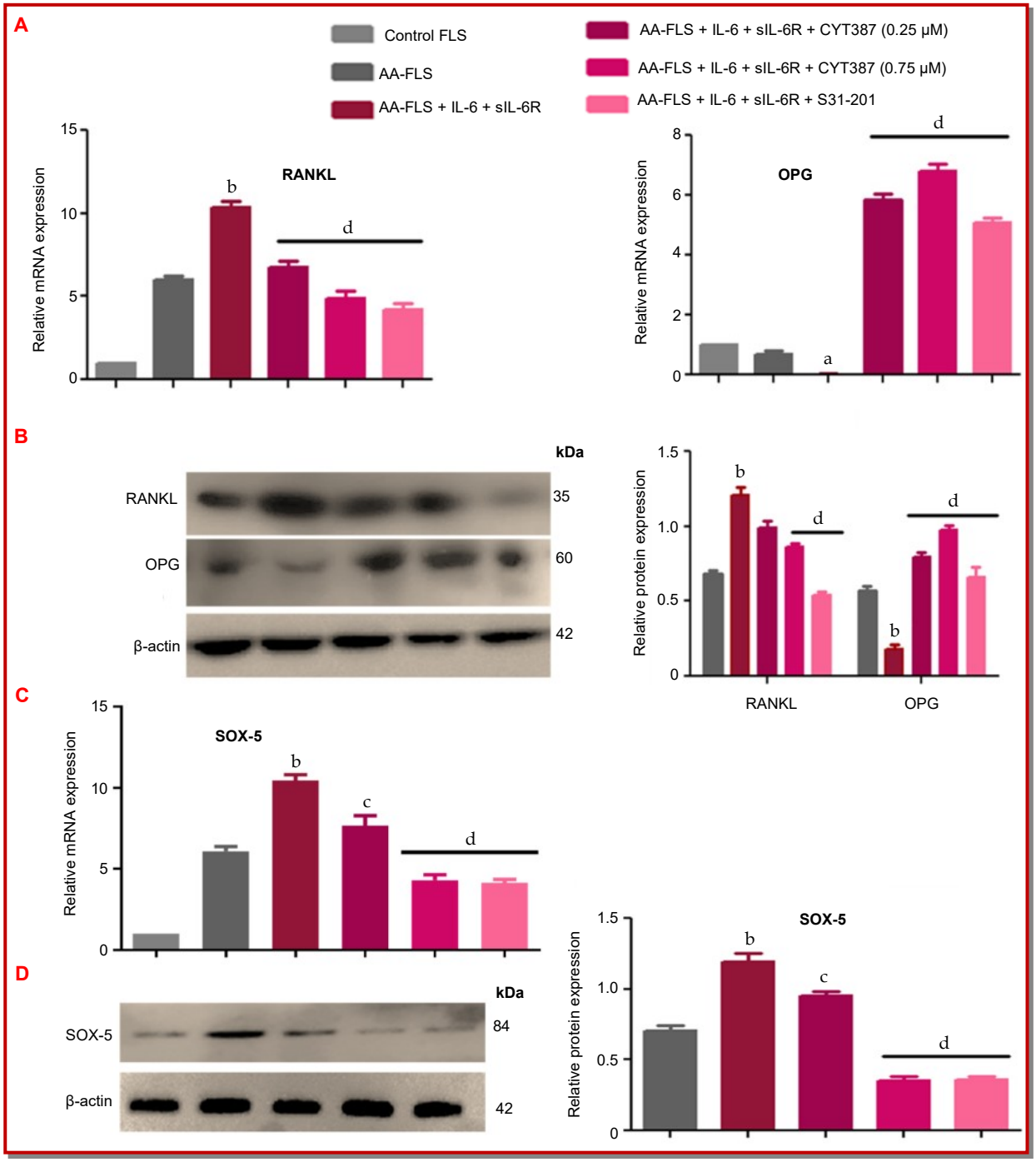


Figure 6: Expression of IL-6/sIL-6R mediated RANKL and osteoprotegerin via SOX-5 signaling in AA-FLS cells upon CYT387 treatment. (A) The mRNA expression of RANKL and osteoprotegerin was determined using quantitative RT-PCR analysis. (B) Western blot analysis was performed to estimate RANKL and osteoprotegerin protein levels.

IL-6/sIL-6R signaling-dependent SOX-5 activation in AA-FLS upon CYT387 treatment. (C) The mRNA expression of SOX-5 was analysed using quantitative real-time PCR. (D) SOX-5 protein levels were confirmed using western blotting. All error bars represent the mean ± SEM (n=3). $^{a}p<0.05$; $^{b}p<0.001$, compared with disease control AA-FLS cells. $^{c}p<0.01$; $^{d}p<0.001$ compared to AA-FLS cells stimulated with IL-6/sIL-6R

addition, TRAP-positive osteoclast numbers were diminished in AA-FLS, where S3I-201 abrogated STAT-3 activity (Figure 5).

Next, a bone resorption assay was performed to confirm CYT387 as an anti-bone resorptive agent. Simultaneously, as depicted in Figure 5B, a significant num-

ber of resorption pits were observed in AA-FLS stimulated with IL-6 and sIL-6R upon co-culturing with precursor osteoclast cells when compared with the number of pits formed in unstimulated AA-FLS. However, treatment of CYT387 (0.75 µM) predominantly curtailed the IL-6/sIL-6R mediated osteoclastogenic instigating capacity in AA-FLS cells. Moreover, a close depletion in resorbed areas was noted in STAT-3 inactivated IL-6 and sIL-6R stimulated AA-FLS cells when co-cultured with precursor macrophage cells.

***CYT387 represses IL-6/sIL-6R mediated RANKL and osteoprotegerin levels via SOX-5 signaling in AA-FLS cells***

Scientific studies have shown a robust effect of IL-6 on RANKL production in RA-FLS upon STAT3-SOX-5 activation (Feng et al., 2016). The present study highlighted the anti-osteoclastogenic potential of CYT387 by quantifying the levels of RANKL and osteoprotegerin. Concomitantly, IL-6 and sIL-6R stimulation increased the amount of RANKL (Figure 6) and mitigated osteoprotegerin levels in AA-FLS, as seen by qRT-PCR and immunoblotting. Where-as post-treatment of CYT387 (0.75 µM) reduced the RANKL level and heightened the osteoprotegerin levels in AA-FLS. Interestingly, SOX-5 elevated mRNA and protein expression in AA-FLS cells stimulated with IL-6/sIL-6R (Figure 6). Intriguingly, post-treatment with CYT387 (0.75 µM), IL-6, and sIL-6R regulated the expression of SOX-5, which was mainly reduced in AA-FLS. Similar results were noted for STAT-3-inactivated IL-6 and sIL-6R-stimulated AA-FLS cells. Altogether, these reports demonstrate that CYT-387 may halt the differentiation of precursor osteoclast cells into mature osteoclasts, along with bone resorption activity.

## Discussion

IL-6 targeted therapies were found to be highly efficacious in rheumatoid arthritis treatment but are often associated with dysregulated adaptive immune responses (Dayer and Choy 2010; Avci et al.,2018). For example, anti-IL-6 mAb, like tocilizumab, has achieved significant commercial success but accounts for limitations in clinical utility due to its complex molecular structure, invasive route of administration, and tissue accumulation (Shetty et al., 2014; Quartuccio et al., 2018). This paves the way for more attentive and intriguing studies exploring the inhibition of JAK activation to identify potential therapeutic targets for rheumatoid arthritis. JAK inhibitors have demonstrated better clinical efficacy as a radical strategy to abate IL-6 modulated aberrant activity in rheumatoid arthritis. A recent study demonstrated the anti-arthritic potential of CYT387, a JAK1/2 inhibitor, in IL-6 trans-signaling directed fibroblast-like synoviocyte proliferation and migration (Srivastava et al., 2021). Nonetheless, the effect of CYT387 on the IL-6 trans-signaling-mediated disproportion of Th17/Treg cells and osteoclast formation has not been well explored. The present investigation highlights that CYT387 synchronically relocates the balance towards autoimmunity, resisting Treg cells, compared to their pathogenic variant, Th17 cells. Furthermore, CYT387 prevented the differentiation of osteoclast precursors and bone marrow macrophages into mature osteoclasts. These findings may potentiate CYT387 as a cornerstone of rheumatoid arthritis treatment.

Th17 cells are abundant in inflamed synovial joints and aggravate the inflammatory phase of the disease by activating various cells, such as macrophages and fibroblast-like synoviocytes, which later mediate proinflammatory responses (Samarpita et al., 2021). These findings pave the way for the pathogenic involvement of Th17 cells at an early stage of rheumatoid arthritis, where a prominent cytokine, IL-17, which is noticeably released by Th17 cells, has been reported at heightened levels (Samarpita et al., 2021; Le Goff et al., 2019). It plays an influential role in joint inflammation, pannus growth, cartilage degradation, and bone lesions by inducing the secretion of various inflammatory cytokines along with cartilage and bone destruction mediators. Moreover, elevated IL-17 levels have been associated with disease severity and heightened disease activity (Samarpita et al., 2021). The hyperactivated synovium in rheumatoid arthritis patients has also shown increased expression of RORγT via IL-6 trans-signaling, which causes differentiation, migration, and accumulation of Th17 cells, thus causing immune-mediated damage (McLoughlin et al., 2005). However, reduced expression of FOXP3 and its related molecule IL-10 further correlates with impaired Treg cell functionality in the IL-6 microenvironment. This evokes autoimmune responses and leads to chronic inflammation (Yang et al., 2019; Esensten et al., 2009)]. In the present study, CYT387 reformed the disparity of CD4+T cells towards immune homeostasis, maintaining regulatory T cells rather than its pathogenic phenotype. Furthermore, CYT387 effectively reduced IL-17 and augmented IL-10 levels. These data show that IL-6 and sIL-6R mediated asymmetric levels of Th17/Treg can be a possible mechanistic target for CYT387 in abrogating the pathological responses in the adjuvant-induced arthritic model of rheumatoid arthritis. Consequently, CYT387 also reduced IL-23R expression, which halted its interaction with IL-23, thereby diminishing the maturation of Th17 cells.

Alongside impaired Th17/Treg balance, bone loss mediated by mature osteoclasts is also a notable detrimental feature of the disease. The interplay between an array of chemokines and other variable factors attracts osteoclast precursors at the resorption site and differentiates them into mature, multinucleated osteoclast cells via osteoclastogenesis (Feng et al., 2016). When ligated with a RANK receptor on precursor cells

in the IL-6/sIL-6R microenvironment of inflamed synovium, RANKL enhances osteoclast formation and subsequent survival. Reports have shown that augmented RANKL and diminished osteoprotegerin levels in rheumatoid arthritis patients consequently activate signaling cassettes to drive osteoclastogenesis, ultimately causing bone erosion (Singh et al., 2021). Consistent with these findings, the current study showed increased osteoclast formation and bone resorption in AA-FLS upon IL-6 and sIL-6R stimulation via magnified RANKL production and reduced osteoprotegerin levels. Correspondingly, in AA-FLS, CYT387 treatment functionally mitigated RANKL production and increased osteoprotegerin levels in the IL-6/sIL-6R microenvironment. Additionally, STAT-3 blockade by S3I-201 also demonstrated similar results. In line with this, CYT387 treatment of the co-culture of AA-FLS and bone marrow-derived macrophages reduced the number of TRAP+ osteoclasts and the pit forming activity of mature osteoclasts. The diminished expression of RANKL in AA-FLS cells halted the maturation of precursor osteoclasts to mature TRAP+ osteoclasts. Overall, the present findings highlighted CYT387's anti-bone resorption activity in AA-FLS cells by modulating the IL-6/sIL-6R/JAK1/STAT-3 signaling pathway.

RORγT has already been recognized as a lineage-specifying modulator of Th17 cell differentiation and the subsequent release of its primary cytokine, IL-17 (Samarpita et al., 2021). A recent study illustrated that SOX-5, along with c-Maf, is a crucial factor in RORγT induction, which further leads to the differentiation of Th17 cells (Tanaka et al., 2014). Various studies have confirmed that STAT-3 is also indispensable for RORγT expression during Th17 cell differentiation. Recent reports have suggested that IL-6-mediated STAT-3 signaling is also critical for inducing downstream activation of SOX-5 and c-Maf transcriptional factors (Tanaka et al., 2014). Based on these findings, this study evaluated the pivotal role of IL-6 trans-signaling, which leads to the aberrant functionality of the JAK-1/STAT-3/ SOX-5/c-Maf signaling cascade in CD4+T cells isolated from arthritis-induced rats, leading to the initiation of pathogenic Th17 cells. Concomitantly, overexpression of SOX-5 is seen in rheumatoid arthritis-FLS, which demonstrates an influential role in modulating RANKL levels via enhanced binding to the promoter region (Feng et al., 2016). Nonetheless, the roles of IL-6 and sIL-6R in SOX-5 expression, which ultimately affects RANKL expression, are presented in this study. Consequently, blocking the activity of IL-6/sIL-6R regulates SOX-5 by inhibiting JAK-1/STAT-3 activation, which can reverse the differentiation of CD4+ T cells into Treg cells and restore the balance between Th17 and Treg cells. Similarly, reducing IL-6/sIL-6R mediated, SOX-5 levels can also be intricate in abrogating the excessive production of RANKL in RA. As expected, CYT387 markedly reduced the expression of SOX-5, thus inhibiting the differentiation of CD4+ T cells towards the Th17 phenotype. Under Th17 polarizing conditions and in the presence of sIL-6R, CYT387 altered IL-6 trans-signaling-mediated up-regulation of intracellular protein JAK-1 and the subsequent downstream transcription factor STAT-3 in CD4+T cells from experimental arthritis rats. Moreover, upon CYT387 treatment, the differentiation of Th17 cells upon sIL-6R stimulation was diminished through the down-regulation of RORγT expression. Subsequently, CYT387 treatment induced Treg differentiation by up-regulating FOXP3. Similarly, upon CYT387 treatment, the reduced expression of SOX-5 and c-Maf indicated that these are the main effector molecules downstream of the IL-6/sIL-6R/JAK1/STAT3 pathway, which up-regulates RORγT expression. Second, as a pivotal mediator of bone damage, RANKL orchestrates osteoclast differentiation.

Concomitantly, our data suggested that CYT387 abrogated SOX-5 levels in AA-FLS cells, thus showcasing itself as a potent anti-bone resorptive agent by regulating IL-6/sIL-6R/JAK-1/STAT-3 signaling, which relies on RANKL levels along with osteoprotegerin. CYT387 also increased SOCS-3 protein expression, an important JAK-1 inhibitor. Further, CYT387 interferes with the phosphorylation and activation of JAK-1/STAT-3 and SOX-5 upon IL-6 and sIL-6R stimulation, thus indicating its restraining effect via the IL-6/sIL-6R/JAK-1/STAT-3/SOX-5 signaling pathway.

## Conclusion

CYT387 prevents the differentiation and maturation of antigen-activated CD4+T cells into Th17 cells by mitigating the levels of important inducible mediators and also sheds light on the anti-osteoclastogenic potential of CYT387.

## Financial Support

Self-funded

## Ethical Issue

All experiments were certified and reviewed by the Institutional Animal Ethical Committee members (approval number: VIT/IAEC/18/Dec2020/14). All experimental procedures were performed according to the guidelines proposed by the Committee for Control and Supervision of Experiments on Animals in New Delhi, India.

## Conflict of Interest

Authors declare no conflict of interest

## References


Avci AB, Feist E, Burmester GR. Targeting IL-6 or IL-6 receptor in rheumatoid arthritis: What's the Difference? BioDrugs. 2018; 32: 531-46

Bin Dhuban K, Bartolucci S, d'Hennezel E, Piccirillo CA. Signaling through gp130 compromises suppressive function in human FOXP3+ regulatory T cells. Front Immunol. 2019; 2019.

Chen HL, Lin SC, Li S, Tang KT, Lin CC. Alantolactone alleviates collagen-induced arthritis and inhibits Th17 cell differentiation through modulation of STAT3 signalling. Pharm Biol. 2021; 59; 132-43.

Dayer JM, Choy E. Therapeutic targets in rheumatoid arthritis: The interleukin-6 receptor. Rheumatology (Oxford). 2010; 49: 15-24.

Esensten JH, Wofsy D, Bluestone JA. Regulatory T cells as therapeutic targets in rheumatoid arthritis. Nat Rev Rheumatol. 2019; 5: 560-65.

Feng X, Shi Y, Xu L, Peng Q, Wang F, Wang X, Sun W, Lu Y, Tsao BP, Zhang M, Tan W. Modulation of IL-6 induced RANKL expression in arthritic synovium by a transcription factor SOX5. Sci Rep. 2016; 6: 32001.

Gupta V, Mesa RA, Deininger MW, Rivera CE, Sirhan S, Brachmann CB, Colins H, Kawashima J, Xin Y, Verstovsek S. A phase 1/2, open-label study evaluating twice-daily administration of momelotinib in myelofibrosis. Haematologica 2017; 102: 94-102.

Hashizume M, Hayakawa N, Mihara M. IL-6 trans-signalling directly induces RANKL on fibroblast-like synovial cells and is involved in RANKL induction by TNF-alpha and IL-17. Rheumatology (Oxford). 2008; 47: 1635-40.

Jiang Q, Yang G, Liu Q, Wang S, Cui D. Function and role of regulatory T cells in rheumatoid arthritis. Front Immunol. 2021; 12: 626193.

Jones GW, McLoughlin RM, Hammond VJ, Parker CR, Williams JD, Malhotra R, Scheller J, Williams AS, John SR, Topley N, Jones SA. Loss of CD4+ T cell IL-6R expression during inflammation underlines a role for IL-6 trans signaling in the local maintenance of Th17 cells. J Immunol. 2010; 184: 2130-39.

Kim J, Kang S, Kim J, Kwon G, Koo S. Elevated levels of T helper 17 cells are associated with disease activity in patients with rheumatoid arthritis. Ann Lab Med. 2013; 33: 52-59.

Kimura A, Kishimoto T. IL-6: Regulator of Treg/Th17 balance. Eur J Immunol. 2010; 40: 1830-35.

Kondo N, Kuroda T, Kobayashi D. Cytokine networks in the pathogenesis of rheumatoid arthritis. Int J Mol Sci. 2021; 22: 10922.

Kotake S, Yago T, Kobashigawa T, Nanke Y. The plasticity of Th17 cells in the pathogenesis of rheumatoid arthritis. J Clin Med. 2017; 6: 67.

Le Goff B, Bouvard B, Lequerre T, Lespessailles E, Marotte H, Pers YM, Cortet B. Implication of IL-17 in bone loss and structural damage in inflammatory rheumatic diseases. Mediators Inflamm. 2019; 2019.

McInnes IB, Buckley CD, Isaacs JD. Cytokines in rheumatoid arthritis-shaping the immunological landscape. Nat Rev Rheumatol. 2016; 12: 63-68.

McLoughlin RM, Jenkins BJ, Grail D, Williams AS, Fielding CA, Parker CR, Ernst M, Topley N, Jones SA. IL-6 trans-signaling via STAT3 directs T cell infiltration in acute inflammation. Proc Natl Acad Sci USA. 2005; 102: 9589-94.

Noack M, Miossec P. Th17 and regulatory T cell balance in autoimmune and inflammatory diseases. Auto-immun Rev. 2014; 13: 668-77.

Quartuccio L, Zabotti A, Del Zotto S, Zanier L, De Vita S, Valent F. Risk of serious infection among patients receiving biologics for chronic inflammatory diseases: Usefulness of administrative data. J Adv Res. 2018; 15: 87-93.

Samarpita S, Rasool M. Cyanidin restores Th17/Treg balance and inhibits T follicular helper cell differentiation via modulation of ROCK2 signaling in an experimental model of rheumatoid arthritis. Int Immunopharmacol. 2021; 101: 108359.

Shetty A, Hanson R, Korsten P, Shawagfeh M, Arami S, Volkov S, Vila O, Swedler W, Shunaigat AN, Smadi S, Sawaged R, Perkins D, Shahrara S, Sweiss NJ. Tocilizumab in the treatment of rheumatoid arthritis and beyond. Drug Des Devel Ther. 2014; 8: 349-64.

Singh AK, Haque M, Madarampalli B, Shi Y, Wildman B, Basit A, Khuder SA. Prasad B, Hassan Q, Quseph MM, Ahmed S. Ets-2 Propagates IL-6 trans-signaling mediated osteoclast-like changes in human rheumatoid arthritis synovial fibroblast. Front Immunol. 2021; 12: 746503.

Srivastava S, Samarpita S, Ganesan R, Rasool M. CYT387 inhibits the hyperproliferative potential of fibroblast-like synoviocytes via modulation of IL-6/JAK1/STAT3 signaling in rheumatoid arthritis. Immunol Invest. 2022; 51: 1582-97.

Tanaka S, Suto A, Iwamoto T, Kashiwakuma D, Kagami SI, Suzuki K, Takatori H, Tamcahi T, Hirose K, Onodera A, Suzuki J, Ohara O, Yamashimita M, Nakayama T, Nakajima H. Sox5 and c-Maf cooperatively induce Th17 cell differentiation via RORγt induction as downstream targets of Stat3. J Exp Med. 2014; 211: 1857-74.

Tefferi A, Barraco D, Lasho TL, Shah S, Begna KH, Kali AA, Hogan WJ, Litzow MR, Hanson CA, Ketterling RP, Gangat N, Pardanani A. Momelotinib therapy for myelofibrosis: A 7-year follow-up. Blood Cancer J. 2018; 8: 29.

Toh ML, Miossec P. The role of T cells in rheumatoid arthritis: New subsets and new targets. Curr Opin Rheumatol. 2007; 19: 284-88.

Tymoszuk P, Petzer V, Asshoff M. SAT0020 Momelotinib, a janus kinase ½ and activin receptor 1 inhibitor ameliorates joint inflammation, systemic TH17 differentiation and arthritis-linked anemia in preclinical autoimmune RA. Ann Rheum Dis. 2020; 940.

Van Hamburg JP, Tas SW. Molecular mechanisms underpinning T helper 17 cell heterogeneity and functions in rheumatoid arthritis. J Autoimmun. 2018; 87: 69-81.

Verstovsek S, Chen CC, Egyed M, Ellis M, Goh YT, Gupta V, Harrison C, Kiladjian JJ, Lazariou M, Mead A, Mclornan D,

McMullin MF, Oh ST, Perkins A, Platzbecker L, Schied C, Vannuchi A, Yoon SS, Kowalski MM, Mesa R. Momelotinib: Momelotinib vs danazol in patients with myelofibrosis previously treated with JAKi who are symptomatic and anemic. Future Oncol. 2021; 17: 1449-58.

Wu Q, Zhou X, Huang D. IL-6 Enhances osteocyte-mediated osteoclastogenesis by promoting JAK2 and RANKL activity *in vitro*. Cell Physiol Biochem. 2017; 41: 1360-69.

Yang P, Qian FY, Zhang MF, Xu AL, Wang X, Jiang BP, Zhou LL. Th17 cell pathogenicity and plasticity in rheumatoid arthritis. J Leukoc Biol. 2019; 106: 1233-40.

Yang XO, Panopoulos AD, Nurieva R, Chang SH, Wang D, Watowich W, Dong C. STAT3 regulates cytokine-mediated generation of inflammatory helper T cells. J Biol Chem. 2007; 282: 9358-63.

**Author Info**
Mahaboobkhan Rasool (Principal contact)
e-mail: rasool.m@vit.ac.in